HHS Public Access

Author manuscript

Exp Eye Res. Author manuscript; available in PMC 2022 October 01.

Published in final edited form as:

Exp Eye Res. 2021 October ; 211: 108762. doi:10.1016/j.exer.2021.108762.

Evidence for Ceramide induced Cytotoxicity in Retinal Ganglion Cells

Jie Fan[1,*,†], **Jiali Liu**[2,†], **Jian Liu**[1], **Chunhe Chen**[1], **Yiannis Koutalos**[1], **Craig E Crosson**[1]

[1]Storm Eye Institute, Medical University of South Carolina, Department of Ophthalmology, 167 Ashley Ave, Charleston, SC 29425

[2]Shanghai Municipal Hospital of Traditional Chinese Medicine, Shanghai University of Traditional Chinese Medicine, Department of Ophthalmology, 274 Middle Zhijiang Road, Jingan District, Shanghai, 200071 China

Abstract

Ceramides are bioactive compounds that play important roles in regulating cellular responses to extracellular stimuli and stress. Previous studies have shown that ceramides contribute to retinal degeneration associated with ischemic and ocular hypertensive stress. Acid sphingomyelinase (ASMase) is one of the major enzymes responsible for the stress-induced generation of ceramides. The goals of this study are to investigate the effects of ceramides on retinal ganglion cells (RGCs) and of ASMase inhibition in ocular hypertensive mice. Induced pluripotent stem cell (iPSC)-derived RGCs and primary cultures of human optic nerve head astrocytes were used to characterize the response to C2-ceramide. Microbead-induced ocular hypertension in the ASMase heterozygote mouse model was used to confirm the physiological relevance of *in vitro* studies. In mice, RGC function and morphology were assessed with pattern ERG (pERG) and immunofluorescence. The addition of C2-ceramide to iPSC-derived RGCs produced a significant concentration- and time-dependent reduction in cell numbers when compared to control cultures. While the addition of C2-ceramide to astrocytes did not affect viability, it resulted in a 2.6-fold increase in TNF-α secretion. The addition of TNF-α or conditioned media from C2-ceramide-treated astrocytes to RGC cultures significantly reduced cell numbers by 56.1 ± 8.4% and 24.7 ± 4.8%, respectively. This cytotoxic response to astrocyte-conditioned media was blocked by TNF-α antibody. In ASMase heterozygote mice, functional and morphological analyses of ocular hypertensive eyes reveal significantly less RGC degeneration when compared with hypertensive eyes from wild-type mice. These results provide evidence that ceramides can induce RGC cell death by acting directly, as well as indirectly via the secretion of TNF-α from optic nerve head astrocytes. *In vivo* studies in mice provide evidence that ceramides derived through the activity of ASMase contribute to ocular hypertensive injury. Together these results support the importance of ceramides in the pathogenesis of ocular hypertensive injury to the retina.

[*]Corresponding author: Jie Fan, PhD, fan@musc.edu, Medical University of South Carolina, Department of Ophthalmology, 167 Ashley Ave, Charleston, SC 29425.

[†]Co-first authors

Keywords

glaucoma; stem cell; retinal ganglion cells; ceramide; TNF-α; astrocytes

1. INTRODUCTION

Glaucoma is the second leading cause of blindness worldwide (Resnikoff et al., 2004). Morphological glaucoma is characterized as an optic neuropathy associated with thinning of the nerve fiber layer and cupping of the optic disc that results from the degeneration of retinal ganglion cells (RGCs) and their axons (Quigley and Green, 1979). Current treatments for glaucoma are based mainly on pharmacological, surgical or laser-based approaches that aim to lower the intraocular pressure (IOP). However, many studies have shown that IOP reduction is not always feasible or effective; moreover, RGC loss still progresses even when IOP is maintained at normal levels (Fernandes et al., 2015). As the prevention of RGC loss is the therapeutic goal in glaucoma, it is important to characterize the events leading to RGC degeneration.

Ceramides are a family of sphingolipids that play important roles in regulating cellular responses to extracellular stimuli and stress (Hannun and Obeid, 2008). Ceramides can be generated through three major pathways (Kitatani et al., 2008): (1) *de novo* ceramide synthesis through a series of reactions, (2) salvage pathway, which recycles the long-chain sphingoid bases through the actions of ceramide synthases, (3) hydrolysis pathway, catalyzed by sphingomyelinase (SMase) enzymes. Sphingomyelinases breakdown sphingomyelin to generate ceramide; studies have shown that changes in acid sphingomyelinase (ASMase) activity contribute to the sequence of events leading to inner retinal degeneration in ischemic eyes (Fan et al., 2016b). Inhibition of neutral sphingomyelinase has been shown to limit RGC loss in ocular hypertensive rodents (Aslan et al., 2014). The purpose of this study is to investigate whether ceramides affect RGC and optic nerve head astrocyte viability and if reducing ASMase expression can protect RGCs from ocular hypertensive stress *in vivo*.

Recently, retinal neurons derived from human induced pluripotent stem cells (iPSCs) have been used as model systems for many human retinal diseases (Jayakody et al., 2015; Sluch and Zack, 2014; Wahlin et al., 2014). Multiple groups have successfully generated iPSC-derived RGCs using different protocols (Ohlemacher et al., 2016; Sluch et al., 2017; Tanaka et al., 2016). We generated iPSC-derived RGCs according to published protocols (Ohlemacher et al., 2015), further purified them, and used them as an *in vitro* model system for evaluating ceramide-induced cytotoxicity. In addition, we utilized primary cultures of human optic nerve head astrocytes to investigate the actions of ceramides on these cells.

Rodent models have been widely used for studying the mechanisms of RGC degeneration and glaucomatous retinal diseases (Fan et al., 2016a; Morgan and Tribble, 2015; Sappington et al., 2010). The microbeads occlusion model mimics the clinical condition in glaucoma: microbeads injected into the anterior chamber disrupt the outflow of aqueous humor resulting in a sustained elevation of IOP, which subsequently leads to the loss of RGCs. In our study, we injected magnetic microbeads, and used a magnetic ring to secure them at

the iridocorneal angle to block the drainage of aqueous humor from the anterior chamber and elevate IOP.

Our results demonstrate that ceramides act directly to induce (a) RGC death and (b) the secretion of TNF-α from optic nerve head astrocytes, providing evidence that locally generated ceramides in the RGCs and optic nerve can make a significant contribution to the pathogenesis of glaucomatous optic neuropathy. *In vivo* studies support the idea that ceramides generated by ASMase play a central role in these events *in vivo*.

2. METHODS AND MATERIALS

2.1. Human iPSC-derived RGCs

Human iPSC cells were purchased from WiCell Research Institute (Madison, WI) and thawed following the manufacturer's instructions. Cells were maintained in mTeSR1 media (Stemcell Technologies, MA) on growth factor-reduced Matrigel (Corning, AZ) coated plates. Confluent cells were passaged and lifted with dispase (Life Technologies/Thermo Fisher Scientific, CA) treatment for 3 minutes in DMEM/F12. Cell suspensions were centrifuged at 150 × g for 6 min and cell pellets were resuspended in mTeSR1. Media were changed daily.

Human iPSC-derived RGCs were generated from human pluripotent stem cells following published procedures (Ohlemacher et al., 2015). Briefly, the iPSCs were directed to differentiate into retina cells in a step-wise process by generation of embryoid bodies. After 7 total days of differentiation, embryoid bodies were plated and adherent cultures maintained for a total of 16 days. Neurospheres were generated and retinal progenitor cell population was enriched by manually selecting retinal neurospheres with the appearance of a golden ring around the outside by day 25 and cultured for at least an extra 25 days.

Retinal neurospheres differentiated for 50-55 days were collected and dissociated by accutase (Sigma-Aldrich, MO) and incubated with CD90.2 (THY1.2) microbeads (Miltenyi Biotec, Germany) for 20 minutes at 4 °C. The cells were purified by using the MACS MS column (Miltenyi Biotec, Germany) following the manufacturer's instructions. Purified cells were cultured overnight in BrainPhys™ Neuronal medium (Stem Cell Technologies, Canada) including B27 supplement (Thermo Fisher Scientific, MA) on the Matrigel (Corning, AZ) coated slides.

2.2. RGC Characterization

Total RNA was extracted using the RNeasy Mini kit (QIAGEN, MD). Extracted RNA was reverse transcribed using the Superscript II Reverse Transcription Kit (Invitrogen). qPCR was performed using the following program: 90°C, 60°C, and 72°C for 40 Cycles. All assays included triplicates in 20 μl reactions using the SYBR Green (Bio-Rad) and 1 μM oligonucleotide primers (Integrated DNA Technologies,Inc, IA). Primers used were:

Brn3 forward: CTCACACTGTCCCACAATAATA

Brn3 reverse: CCGGCGGAATATTTCATTCT

CD90 forward: AGAGACTTGGATGAGGAG

CD90 reverse: CTGAGAATGCTGGAGATG

Islet1 forward: GTGTGATCCGGGTCTGGTTT

Iselt1 reverse: AATTAGAGCCCGGTCCTCCT

CHX10 forward: ATTCAACGAAGCCCACTACCCAGA

CHX10 reverse: ATCCTTGGCTGACTTGAGGATGGA

ATOH7 forward: CCCTAAATTTGGGCAAGTGAAGA

ATOH7 reverse: CAAAGCAACTCACGTGCAATC

GAPDH forward: ACCACAGTCCATGCCATCAC

GAPDH reverse: TCCACCACCCTGTTGCTGTA

PAX6 forward: CGG AGT GAA TCA GCT CGG TG

PAX6 reverse: CCG CTT ATA CTG GGC TAT TTT GC

RPE65 forward: TAC CAC AGA AGG TTC ATC CGC ACT

RPE65 reverse: GGG AAA GCA CAG GTG CCA AAT TCT

Gene expression of each sample was normalized to the mean values of the reference gene GAPDH.

2.3. C2-ceramide and TNF-α Toxicity Assay

Purified iPSC-derived RGCs were treated with C2-ceramide (0.3, 1, 3 and 10 μM) (Sigma-Aldrich, MO) or TNF-α (5, 50, 500 ng/ml) (R&D Systems, MN) for 24 or 48 hours. When testing the indirect response from C2-ceramide, astrocytes were treated with 10 μM C2-ceramide for 24 hours, then media were collected and fed to iPSC-derived RGC cultures with or without the TNF-α antibody (BioLegend, CA, 1:50) for 24 hours. Subsequently, cells were fixed with 4% PFA for immunofluorescence staining. Only Brn3a or βIII-tubulin positive cells were used for data analysis.

2.4. Astrocyte Culture

Primary human optic nerve head astrocytes were isolated and cultured as previously described (Yang and Hernandez, 2003). Confluent astrocyte cultures were serum-starved overnight and then treated with C2-ceramide (10 μM). Media were collected after a 24 hour-incubation for experiments with RGCs or for TNF-α ELISA analysis.

2.5. TNF-α Analysis

Astrocyte culture media were collected and used to measure TNF-α with a commercial ELISA kit following the manufacturer's instructions (eBioscience, San Diego, CA).

2.6. Measurement of Ca^{2+}-dependent fluorescence change

Ca^{2+} dependent fluorescence was measured following procedures described previously (Nakatani et al., 2002), with appropriate modifications for mammalian cells. Briefly, the cells were maintained in a physiological solution (130 NaCl, 5 KCl, 0.5 $MgCl_2$, 2 $CaCl_2$, 25 hemisodium-HEPES, 5 glucose, pH = 7.40) and loaded with fluo-3-AM for 30 min in a chamber dish at room temperature. Excess dye was washed off, and the chamber containing the cells was placed on the stage of an inverted Zeiss Axiovert 100 microscope (Carl Zeiss, Thornwood, NY). Cells were imaged using an oil immersion Zeiss 40× Plan Neofluar (NA=1.3). The experiments were carried out at 37 °C.

2.7. Immunofluorescence staining for RGC and astrocytes

Cells were fixed in 4% paraformaldehyde for 15 minutes, permeabilized and blocked in 0.1% Triton X-100 in PBS with 3% bovine serum albumin and 3% normal goat serum and for 1 hour at room temperature, and then incubated with primary antibody overnight at 4 °C. Primary antibodies used were Brn3a (Santa Cruz, TX, 1:200), βIII-tubulin (Thermo Scientific, MA 1:500), GFAP (Sigma-Aldrich, MO, 1:500), ASMase H181 (Santa Cruz, TX, 1:500). Cells were incubated with corresponding secondary antibodies for 2 hours at room temperature. DAPI (ThermoFisher Scientific, MA, 1:1000) was used to stain nuclei. Fluorescence images were acquired with a Nikon A1Rsi confocal microscope with 20x and 60x objective lenses (Fig.4) and Leica confocal microscope with 20x objective lens (Fig.3). We found two types of cells after purification with Thy 1.2 coated microbeads. The majority of cells are RGCs, on the basis of their expressing Brn3a and βIII-tubulin. Some cells also express Thy 1.2 but display distinct morphology: the size of their nuclei are 2-4 time larger than RGC nuclei, do not express Brn3a or βIII-tubulin, and do not have typical neurites. Only Brn3a and βIII-tubulin positively-stained cells were used for assessing RGC responses in this study.

2.8. Animals

The ASMase knockout mice on a C57/BL6 background were the generous gift of Edward H. Schuman (Icahn Medical Institute, New York, NY). Heterozygous ($ASMase^{+/-}$) mice were bred and genotyped as previously described (Horinouchi et al., 1995). Mice 10 to 12 weeks of age were used for the experiments. Because previous studies have shown that ASMase homozygous knockout mice exhibit outer retinal dysfunction and degeneration (Wu et al., 2015), $ASMase^{+/-}$ mice were used for the experiments in this study. All experiments were performed in accordance with the ARVO Statement for the Use of Animals in Ophthalmic and Vision Research; the study protocol was approved by the MUSC Animal Care and Use Committee.

2.9. Intraocular Pressure Elevation and Measurement

Intraocular pressure (IOP) was elevated unilaterally in mice (10-12 weeks) with microbead injection as described previously (Bunker et al., 2015; Ito et al., 2016) with some modifications. Briefly, mice were anesthetized with ketamine and xylazine (90 mg/kg and 10 mg/kg) injected intraperitoneally. Corneas were anesthetized by topical application of 0.5% proparacaine. Magnetic microbeads (8 μm, 5μl of 30mg/ml solution, 5 X 10^5

microbeads/eye; Bangs Laboratories, Inc) were injected into the anterior chamber using a glass micro-pipette. A magnetic ring was placed around the eye to direct the microbeads to the iridocorneal angle. The contralateral eye was injected with an equivalent volume of sterile saline and served as control.

Mice were anesthetized with an isoflurane vaporizer (2.5%) (VetEquip Inc. CA) before IOP measurement. As anesthetics can effect IOP (Ding et al., 2011), the duration and level of anesthesia was strictly controlled and all IOP measurements were taken 2 minutes after the induction of anesthesia. IOP for each eye was determined by means of TonoLab rebound tonometer (iCare, Vantaa, Finland). IOP was measured 1 to 3 days prior to bead injection (day 0), and on post-injection days 4, 7, 11, 14, 17, 22 and 28. As all mice exhibited slow but variable declines in IOP over the 28 days study period, integrated IOP was used as a measure of total IOP stress for each animal. Integrated IOP was calculated using procedures originally described by Alsarraf and colleagues (Alsarraf et al., 2014).

2.10. Pattern Electroretinogram

Baseline pERG was recorded one day prior to microbead injection and at 4 weeks following injection with the UTAS-2000 (LKC Technologies, Gaithersburg, MD, USA) as described by Alsarraf and colleagues (Alsarraf et al., 2014). For pERG measurements, mice were anesthetized with ketamine (90 mg/kg) and xylazine (10 mg/kg), and body temperature was maintained at 37°C with a heating pad. The pERG electrode was placed on the corneal surface and positioned to encompass the pupil without limiting the field of view. A visual stimulus was generated by black and white alternating contrast reversing bars (mean luminance, 50 cd/m^2; spatial frequency, 0.033 cyc/deg; contrast, 100%; and temporal frequency, 1 Hz) and was aligned with the projection of the pupil and visual axis at a distance of 11 cm from the center of the screen. Each pERG reading was recorded as an average of 300 sweeps at an interval of 1 second.

2.11. Retinal Flatmount

Mice were sacrificed on day 29 after microbead injection, retinas, lens and vitreous were isolated together from the rest of the eye and fixed in 4% paraformaldehyde at 4°C for 2 hours. Retinas were separated from lenses, flattened on a cover slip and permeabilized with 0.5% Triton X-100 in PBS at −70°C for 5 min and incubated in blocking buffer (PBS with 2% donkey serum and 2% Triton X-100) at room temperature for 1 hour; they were then incubated with primary antibody Brn3a (Santa Cruz, 1:200) overnight at 4 °C, followed with incubation with the corresponding secondary antibodies for 2 hours at room temperature. Fluorescence images were acquired with an Axioplan Zeiss microscope using 20x objective lens. Each retina was divided into four quadrants. Images were taken from peripheral region on each quadrant. RGCs were counted manually by two operators in a masked fashion and confirmed by Image J software.

2.12. Statistics

For all experiments, data are expressed as mean ±SEM. Statistical significance was tested using two-tailed Student *t* test or ANOVA. A $P<0.05$ was considered statistically significant.

3. RESULTS

3.1. Characterization of iPSC-derived RGCs

To characterize and confirm the progression of the cultured stem cells toward RGCs, we examined the expression of relevant retinal transcription factors and RGC markers by quantitative real time PCR (qPCR) over a period of 60 days (Figure 1A). PAX6 is essential for morphogenesis of the visual system (Gehring, 1996; Nishina et al., 1999) and CHX10 is required for retinal progenitor cell proliferation (Burmeister et al., 1996). Upregulation of PAX6 and CHX10 was detected at days 7 and 20, respectively. Additionally, we examined the time course of the expression of ATOH7, Brn3, Thy1 and Islet1. ATOH7 (also known as MATH5 in mouse) is expressed in progenitors of all retinal cell types (Brzezinski et al., 2012) and is essential for RGC fate (Brown et al., 2001; Wang et al., 2001). Islet1 interacts with the common RGC marker Brn3b to co-regulate genes involved in RGC differentiation (Badea and Nathans, 2011; Bryant et al., 2002; Li et al., 2014). ATOH7, Islet1 and Brn3 expression were detected starting on day 30.

In order to enrich the population of differentiated stem cells with RGCs, we collected retinal neurospheres at day 50-55 and purified the dissociated mixed cells using Thy 1.2 coated microbeads. The expression levels of Brn3 and Thy1 in the purified fractions increased 2.2 ± 0.3 and 2.8 ± 0.5 times respectively (n = 4). Immunofluorescence staining for Brn3a and βIII-tubulin indicates that the major cell population in the purified cells are RGCs (Figure 1B).

To confirm whether the iPSC-derived RGCs exhibit the expected physiological properties, the cell response to glutamate stimulation (Figure 1C) was determined. Administration of glutamate (100μM) results in a significant increase in intracellular Ca^{2+} levels, and this increase is blocked by pretreatment with an NMDA receptor antagonist, MK801 (10μM). This result indicates these iPSC-derived RGCs express functional NMDA receptors.

3.2. Responses of RGCs and astrocytes to C2-ceramide

ASMase is expressed in mouse RGCs and optic nerve head region (Fan et al., manuscript in preparation) and is also expressed in human iPSC-derived RGCs (Figure 2A) and optic nerve head astrocytes (Figure 2B). To examine the effect of ceramides on RGC viability, we evaluated ceramide-induced cytotoxicity in human iPSC-derived RGCs. Enriched RGCs were treated with C2-ceramide, a cell-permeable analog of ceramide. Treatment with C2-ceramide resulted in a significant concentration- and time-dependent decrease in RGC numbers, with the loss ranging from 7.3 ± 5 to 68.0 ± 8% (Fig. 2C). The EC_{50}S for this response at 24 and 48 hours were 1.95μM and 2.46μM, respectively.

The addition of C2-ceramide to human optic nerve head astrocytes did not significantly affect astrocyte viability, at concentrations up to 10 μM (data not shown). As TNF-α is a pro-inflammatory cytokine that is synthesized and released from astrocytes and microglia (Moreau et al., 1996; Sawada et al., 2006; Tarkowski et al., 2003), we examined if treatment of primary human optic nerve head astrocytes with C2-ceramide induced the release of TNF-α. As shown in Figure 2D, treatment with C2-ceramide for 6 hours resulted in a significant dose-dependent secretion of TNF-α. The EC_{50} for this response was 0.27μM.

3.3. Response of RGCs to TNF-α

Previous studies have shown that exogenous TNF-α is deleterious to RGCs in both *in vivo* and *in vitro* models (Hong et al., 2009; Kitaoka et al., 2006). Treatment with TNF-α significantly reduced RGC survival with an EC_{50} of 0.59 μM (Figure 3A). There was no significant difference in RGC numbers between TNF-α treatments for 24 and 48 hours.

To investigate whether the level of ceramide-induced secretion of TNF-α from astrocytes alters RGC viability, RGCs were cultured for 24 hours with media collected from astrocytes treated with 10 μM C2-ceramide for 24 hours. The number of RGCs exposed to astrocyte-conditioned media was significantly reduced by 24.7± 4.8% (Fig. 3B). The response to astrocyte-conditioned media was significantly suppressed by the addition of TNF-α antibody. There is no significant difference in survival of RGCs between control and TNF- α antibody treated group.

3.4. Reduced ASMase Expression Protects the Retina from Ocular Hypertensive Injury

We have previously shown that ASMase$^{+/-}$ mice have reduced ceramide levels and their retinas display increased resistance to acute ischemic injury (Fan et al., 2016b). Here we examine whether ASMase$^{+/-}$ mouse RGCs also display increased resistance to injury induced by ocular hypertension. In both ASMase$^{+/-}$ and wild-type mice, significant IOP elevation was observed following microbead injection when compared with baseline IOP (Figure 4A and B), peaking on post injection day 7. While IOPs in microbead-injected eyes from both wild-type and ASMase$^{+/-}$ mice remained significantly elevated beyond day 7, all mice exhibited variable declines in IOP above baseline levels during the remaining course of the study. This decline in IOP is in agreement with previous findings from other groups (Morgan and Tribble, 2015; Chen et al., 2018).

In wild-type mice, pERG amplitude was 19.8 ± 2.1 μV, not significantly different from that in ASMase$^{+/-}$ mice, 20.2 ± 0.7 μV. Twenty eight days following vehicle injection, pERG amplitudes in both wild-type (17.35 ± 1.8 μV) and ASMase$^{+/-}$ (18.9 ± 3.9 μV) contralateral eyes exhibited no significant changes in amplitude compared to their respective baseline values. In wild-type mice, 28 days post bead injection, hypertensive eyes exhibited a significant decrease ($P = 0.04$) in mean pERG amplitude to 9.9 ± 1.7 μV when compared with contralateral eyes (Fig. 5). In ASMase$^{+/-}$ mice, 28 days post bead injection, pERG mean amplitude of hypertensive eyes (14.2 ± 1.8 μV) was not significantly altered (P=0.8) when compared to the contralateral eyes.

No significant difference in RGC density was found between wild-type and ASMase$^{+/-}$ vehicle-treated contralateral eyes. In wild-type mice, 28-days post bead injection, there was a significant reduction in the mean RGC density in hypertensive eyes (1672.2 ± 117.7 cells/mm^2; $P < 0.001$) compared to contralateral control eyes (2311.4 ± 122.3 cells/mm^2). In ASMase$^{+/-}$ mice, the mean RGC density in hypertensive eyes was 1982.7 ± 55.1 cells/mm^2, not significantly different ($P = 0.15$) from that in contralateral eyes (2201.3 ± 116.3 cells/mm^2). In both wild-type and ASMase$^{+/-}$ mice RGC density correlated with the cumulative IOP increase (Fig 6E). The slope of RGC density changes in response to IOP elevation in wild-type was significantly greater than in ASMase$^{+/-}$ mice (P= 0.03) (Figure 6E).

4. DISCUSSION

Previous studies have shown that ceramide is a key mediator in the induction of apoptosis in retinal photoreceptors (Chen et al., 2012; German et al., 2006; Sanvicens and Cotter, 2006) and RPE (Barak et al., 2001). In rats, intravitreal C2-ceramide injection has been shown to induce apoptosis in the retinal ganglion cell layer, and activate glial cells (Lou et al., 2017). Suppressing ceramide levels by inhibiting ceramide synthesis significantly preserved photoreceptor structure and function in a retinal ischemia and light damage model (Chen et al., 2013; Fan et al., 2016b; Strettoi et al., 2010), and also prevented RGC degeneration in a glaucoma model (You et al., 2014). Reduced expression of ASMase is associated with decreased ceramide levels and with the protection of the inner retina from ischemic injury (Fan et al., 2016b).

In order to investigate direct and indirect effects of ceramides on RGC viability we used human iPSC-derived RGCs as an *in vitro* model system. To generate iPSC-derived RGCs, we followed a published protocol (Ohlemacher et al., 2015) that eliminates non-retinal cell types and ensures that the finally derived cells originate from a retinal progenitor cell population. We then characterized the finally derived cells with a combination of morphological, phenotypic and physiological measurements. RGCs are normally identified by the expression of the transcription factor Brn3 (Badea and Nathans, 2011; Shi et al., 2013). Brn3 however is expressed in neural cells in general (Badea et al., 2012; Bryant et al., 2002; Weir et al., 2000). Since pluripotent stem cells have the potential to give rise to any cell type, Brn3 by itself is not sufficient to identify cells as RGCs. We therefore confirmed the expression of additional transcription factors, CHX10, ATOH7, Islet1 (Fig. 1A), along with the expression of beta III-tubulin (Fig. 1B). Finally, we demonstrated the presence of functional NMDA receptors (Fig. 1C) to confirm the RGC characteristics for the cells used for these studies.

The ceramide analog C2-ceramide exhibited a concentration- and time-dependent effect on RGC viability. A previous *in vitro* study has shown that administration of C2-ceramide increases caspase-8 and caspase-3 activities and leads to necrotic and apoptotic cell death (Ramos et al., 2003). *In vivo* studies demonstrated that the intravitreal injection of C2-ceramide resulted in the significant death of ganglion cells in rodents (Lou et al., 2017). Our results have shown that treatment with C2-ceramide resulted in a significant concentration- and time-dependent decrease in RGC numbers, and are consistent with previous studies that C2-ceramide induces RGC cytotoxicity.

Retinal ganglion cells are known to interact closely with astrocytes with their survival relying on physical contact (McCaffery et al., 1985): astrocytes facilitate the functional maturation of hPSC-derived RGCs (VanderWall et al., 2019), and astrocyte migration is closely associated with the RGC axons in the developing retina (O'Sullivan et al., 2017). Astrocyte reactivity has been associated with declining RGC health (Formichella et al., 2014; Kuse et al., 2017) and astrocytes secrete cytokines and/or growth factors in response to stress or injury. TNF-α in particular has been suggested to play a critical role in the pathogenesis of RGC degeneration (Fuchs et al., 2005), a suggestion borne out by its large effect on RGC numbers shown in Fig. 3A. TNF-α is abundant in microglia and

astrocytes of glaucomatous optic nerve heads (Yan et al., 2000; Yuan and Neufeld, 2000). In the retina, increases in TNF-α are associated with a variety of pathologic conditions including glaucoma (Ramadan et al., 2006; Yoshida et al., 2004). Expression of TNF-α and its receptor-1 are upregulated in glial cells and RGCs, respectively, of glaucoma patients (Tezel and Wax, 2000). *In vitro*, TNF-α production is increased in glial cells exposed to ischemia or elevated hydrostatic pressure, both of which induced apoptosis in RGCs (Tezel and Wax, 2000). Our previous work (Fan et al., 2016b) also suggested the possibility that the deleterious effects of ceramides on RGC viability may be indirect, mediated through an increase in retinal TNF-α. In the present study, C2-ceramide did not affect the viability of human optic nerve head astrocytes at the tested concentration, but it induced the secretion of TNF-α in a dose-dependent manner (Fig. 2D). This points to the possibility of an indirect ceramide cytotoxicity on RGCs, mediated by TNF-α. Such an indirect effect was demonstrated by the experiments of Fig. 3B, in which media collected from astrocyte cultures treated with 10 μM C2-ceramide drastically reduced RGC numbers. Although we could not exclude the possibility that other cytokines might mediate the cytotoxicity on RGCs, TNF- α is likely a dominant cytokine as RGCs were protected by the presence of a TNF-α antibody (Fig. 3B). We have not examined the basal level of TNF-α in RGCs in current study as it requires large scale purification of RGCs. We plan to address this question in future studies.

Many chronic ocular hypertension models have been developed by impeding the aqueous humor outflow pathway (Dey et al., 2018). Injection of microbeads in the anterior chamber creates a blockage at the trabecular meshwork and elevates IOP, resulting in the degeneration of RGCs and their axons (Samsel et al., 2011; Sappington et al., 2010). In the present studies, the injection of microbeads resulted in a significant elevation of IOP, in agreement with results from other groups (Cone et al., 2012; Guttenplan et al., 2020), although a more sustained elevation has been reported by others (Chen et al., 2011; Ito et al., 2016; Sappington et al., 2010). Variabilities associated with the model have been proposed to be due to differences in genetic background, injection volume, or injection technique among others (Cone et al., 2012; Morgan and Tribble, 2015). IOP can be affected by several factors including strain, age, circadian rhythm (Savinova et al., 2001), tonometer (Kim et al., 2007), as well as the duration and strength of anesthesia (Ding et al., 2011) and such differences may contribute to the different IOP elevation patterns that have been reported. In our studies, we achieved a reproducible elevation of IOP by following a strict injection protocol and carefully controlling the dose and duration of anesthesia.

Previous studies have shown that inhibition of neutral sphingomyelinase can protect ocular hypertension-induced RGC degeneration in rodents (Aslan et al., 2014). In the present work, we have shown that the reduced expression of ASMase also preserves RGCs and their function in an ocular hypertension mouse model (Figs. 5 and 6), further reinforcing the importance of ceramide metabolism for RGC health. Expression of ASMase in both RGCs and optic nerve head astrocytes (Fig. 2) supports the idea that locally generated ceramides via ASMase activation in the RGCs and optic nerve can make a significant contribution to the pathogenesis of glaucomatous optic neuropathy.

In summary, our results provide evidence that ceramides can affect RGC viability both directly and indirectly via the secretion of cytokines from optic nerve head astrocytes. Consistent with these effects of ceramides, in a mouse model of ocular hypertension reduction of ceramide levels through suppression of ASMase expression prevents loss of RGCs and preserves function. The results point to bioactive lipids, such as ceramides, as promising therapeutic targets for the treatment of retinal diseases.

ACKNOWLEDGMENTS

The work was supported by a Medical University of South Carolina College of Medicine Enhancement of Team Science award (JF and YK) and National Eye Institute grant EY014850 (YK).

YK is the Barbara and Stanley Andrie Endowed Chair for Bioengineering and Vision Research, in the Vision SmartState Center of Economic Excellence

Abbreviations:

RGC	retinal ganglion cell
ASMase	acid sphingomyelinase
IOP	intraocular pressure
pERG	pattern electroretinogram

6. REFERENCES

Alsarraf O, Fan J, Dahrouj M, Chou CJ, Yates PW, Crosson CE, 2014. Acetylation preserves retinal ganglion cell structure and function in a chronic model of ocular hypertension. Invest Ophthalmol Vis Sci 55, 7486–7493. 10.1167/iovs.14-14792 [PubMed: 25358731]

Aslan M, Basaranlar G, Unal M, Ciftcioglu A, Derin N, Mutus B, 2014. Inhibition of neutral sphingomyelinase decreases elevated levels of inducible nitric oxide synthase and apoptotic cell death in ocular hypertensive rats. Toxicol Appl Pharmacol 280, 389–398. 10.1016/j.taap.2014.08.026 [PubMed: 25201535]

Badea TC, Nathans J, 2011. Morphologies of mouse retinal ganglion cells expressing transcription factors Brn3a, Brn3b, and Brn3c: analysis of wild type and mutant cells using genetically-directed sparse labeling. Vision Res 51, 269–279. 10.1016/j.visres.2010.08.039 [PubMed: 20826176]

Badea TC, Williams J, Smallwood P, Shi M, Motajo O, Nathans J, 2012. Combinatorial expression of Brn3 transcription factors in somatosensory neurons: genetic and morphologic analysis. J Neurosci 32, 995–1007. 10.1523/JNEUROSCI.4755-11.2012 [PubMed: 22262898]

Barak A, Morse LS, Goldkorn T, 2001. Ceramide: a potential mediator of apoptosis in human retinal pigment epithelial cells. Invest Ophthalmol Vis Sci 42, 247–254. https://iovs.arvojournals.org/article.aspx?articleid=2162208 [PubMed: 11133876]

Brown NL, Patel S, Brzezinski J, Glaser T, 2001. Math5 is required for retinal ganglion cell and optic nerve formation. Development 128, 2497–2508. 10.1242/dev.128.13.2497 [PubMed: 11493566]

Bryant J, Goodyear RJ, Richardson GP, 2002. Sensory organ development in the inner ear: molecular and cellular mechanisms. Br Med Bull 63, 39–57. 10.1093/bmb/63.1.39 [PubMed: 12324383]

Brzezinski J.A.t., Prasov L, Glaser T, 2012. Math5 defines the ganglion cell competence state in a subpopulation of retinal progenitor cells exiting the cell cycle. Dev Biol 365, 395–413. 10.1016/j.ydbio.2012.03.006 [PubMed: 22445509]

Bunker S, Holeniewska J, Vijay S, Dahlmann-Noor A, Khaw P, Ng YS, Shima D, Foxton R, 2015. Experimental glaucoma induced by ocular injection of magnetic microspheres. J Vis Exp. doi: 10.3791/52400

Burmeister M, Novak J, Liang MY, Basu S, Ploder L, Hawes NL, Vidgen D, Hoover F, Goldman D, Kalnins VI, Roderick TH, Taylor BA, Hankin MH, McInnes RR, 1996. Ocular retardation mouse caused by Chx10 homeobox null allele: impaired retinal progenitor proliferation and bipolar cell differentiation. Nat Genet 12, 376–384. doi: 10.1038/ng0496-376 [PubMed: 8630490]

Chen H, Cho KS, Vu THK, Shen CH, Kaur M, Chen G, Mathew R, McHam ML, Fazelat A, Lashkari K, Au NPB, Tse JKY, Li Y, Yu H, Yang L, Stein-Streilein J, Ma CHE, Woolf CJ, Whary MT, Jager MJ, Fox JG, Chen J, Chen DF, 2018. Commensal microflora-induced T cell responses mediate progressive neurodegeneration in glaucoma. Nat Commun 9, 3209. 10.1038/s41467-018-05681-9 [PubMed: 30097565]

Chen H, Tran JT, Brush RS, Saadi A, Rahman AK, Yu M, Yasumura D, Matthes MT, Ahern K, Yang H, LaVail MM, Mandal MN, 2012. Ceramide signaling in retinal degeneration. Adv Exp Med Biol 723, 553–558. 10.1007/978-1-4614-0631-0_70 [PubMed: 22183377]

Chen H, Tran JT, Eckerd A, Huynh TP, Elliott MH, Brush RS, Mandal NA, 2013. Inhibition of de novo ceramide biosynthesis by FTY720 protects rat retina from light-induced degeneration. J Lipid Res 54, 1616–1629. 10.1194/jlr.M035048 [PubMed: 23468130]

Chen H, Wei X, Cho KS, Chen G, Sappington R, Calkins DJ, Chen DF, 2011. Optic neuropathy due to microbead-induced elevated intraocular pressure in the mouse. Invest Ophthalmol Vis Sci 52, 36–44. 10.1167/iovs.09-5115 [PubMed: 20702815]

Cone FE, Steinhart MR, Oglesby EN, Kalesnykas G, Pease ME, Quigley HA, 2012. The effects of anesthesia, mouse strain and age on intraocular pressure and an improved murine model of experimental glaucoma. Exp Eye Res 99, 27–35. 10.1016/j.exer.2012.04.006 [PubMed: 22554836]

Dey A, Manthey AL, Chiu K, Do CW, 2018. Methods to Induce Chronic Ocular Hypertension: Reliable Rodent Models as a Platform for Cell Transplantation and Other Therapies. Cell Transplant 27, 213–229. 10.1177/0963689717724793 [PubMed: 29637819]

Ding C, Wang P, Tian N, 2011. Effect of general anesthetics on IOP in elevated IOP mouse model. Exp Eye Res 92, 512–520. 10.1016/j.exer.2011.03.016 [PubMed: 21457709]

Fan J, Alsarraf O, Chou CJ, Yates PW, Goodwin NC, Rice DS, Crosson CE, 2016a. Ischemic preconditioning, retinal neuroprotection and histone deacetylase activities. Exp Eye Res 146, 269–275. 10.1016/j.exer.2016.03.026 [PubMed: 27060376]

Fan J, Wu BX, Crosson CE, 2016b. Suppression of Acid Sphingomyelinase Protects the Retina from Ischemic Injury. Invest Ophthalmol Vis Sci 57, 4476–4484. 10.1167/iovs.16-19717 [PubMed: 27571014]

Fernandes KA, Harder JM, Williams PA, Rausch RL, Kiernan AE, Nair KS, Anderson MG, John SW, Howell GR, Libby RT, 2015. Using genetic mouse models to gain insight into glaucoma: Past results and future possibilities. Exp Eye Res 141, 42–56. 10.1016/j.exer.2015.06.019 [PubMed: 26116903]

Formichella CR, Abella SK, Sims SM, Cathcart HM, Sappington RM, 2014. Astrocyte Reactivity: A Biomarker for Retinal Ganglion Cell Health in Retinal Neurodegeneration. J Clin Cell Immunol 5. 10.4172/2155-9899.1000188

Fuchs C, Forster V, Balse E, Sahel JA, Picaud S, Tessier LH, 2005. Retinal-cell-conditioned medium prevents TNF-alpha-induced apoptosis of purified ganglion cells. Invest Ophthalmol Vis Sci 46, 2983–2991. 10.1167/iovs.04-1177 [PubMed: 16043875]

Gehring WJ, 1996. The master control gene for morphogenesis and evolution of the eye. Genes Cells 1, 11–15. 10.1046/j.1365-2443.1996.11011.x. [PubMed: 9078363]

German OL, Miranda GE, Abrahan CE, Rotstein NP, 2006. Ceramide is a mediator of apoptosis in retina photoreceptors. Invest Ophthalmol Vis Sci 47, 1658–1668. 10.1167/iovs.05-1310 [PubMed: 16565407]

Guttenplan KA, Stafford BK, El-Danaf RN, Adler DI, Munch AE, Weigel MK, Huberman AD, Liddelow SA, 2020. Neurotoxic Reactive Astrocytes Drive Neuronal Death after Retinal Injury. Cell Rep 31, 107776. 10.1016/j.celrep.2020.107776 [PubMed: 32579912]

Hannun YA, Obeid LM, 2008. Principles of bioactive lipid signalling: lessons from sphingolipids. Nat Rev Mol Cell Biol 9, 139–150. 10.1038/nrm2329 [PubMed: 18216770]

Hong S, Kim CY, Lee JE, Seong GJ, 2009. Agmatine protects cultured retinal ganglion cells from tumor necrosis factor-alpha-induced apoptosis. Life Sci 84, 28–32. 10.1016/j.lfs.2008.10.006 [PubMed: 18992261]

Horinouchi K, Erlich S, Perl DP, Ferlinz K, Bisgaier CL, Sandhoff K, Desnick RJ, Stewart CL, Schuchman EH, 1995. Acid sphingomyelinase deficient mice: a model of types A and B Niemann-Pick disease. Nat Genet 10, 288–293. 10.1038/ng0795-288 [PubMed: 7670466]

Ito YA, Belforte N, Cueva Vargas JL, Di Polo A, 2016. A Magnetic Microbead Occlusion Model to Induce Ocular Hypertension-Dependent Glaucoma in Mice. J Vis Exp, e53731. 10.3791/53731 [PubMed: 27077732]

Jayakody SA, Gonzalez-Cordero A, Ali RR, Pearson RA, 2015. Cellular strategies for retinal repair by photoreceptor replacement. Prog Retin Eye Res 46, 31–66. 10.1016/j.preteyeres.2015.01.003 [PubMed: 25660226]

Kim CY, Kuehn MH, Anderson MG, Kwon YH, 2007. Intraocular pressure measurement in mice: a comparison between Goldmann and rebound tonometry. Eye (Lond) 21, 1202–1209. 10.1038/sj.eye.6702576 [PubMed: 16946746]

Kitaoka Y, Kitaoka Y, Kwong JM, Ross-Cisneros FN, Wang J, Tsai RK, Sadun AA, Lam TT, 2006. TNF-alpha-induced optic nerve degeneration and nuclear factor-kappaB p65. Invest Ophthalmol Vis Sci 47, 1448–1457. 10.1167/iovs.05-0299 [PubMed: 16565378]

Kitatani K, Idkowiak-Baldys J, Hannun YA, 2008. The sphingolipid salvage pathway in ceramide metabolism and signaling. Cell Signal 20, 1010–1018. 10.1016/j.cellsig.2007.12.006 [PubMed: 18191382]

Kuse Y, Tsuruma K, Mizoguchi T, Shimazawa M, Hara H, 2017. Progranulin deficiency causes the retinal ganglion cell loss during development. Sci Rep 7, 1679. 10.1038/s41598-017-01933-8 [PubMed: 28490764]

Li R, Wu F, Ruonala R, Sapkota D, Hu Z, Mu X, 2014. Isl1 and Pou4f2 form a complex to regulate target genes in developing retinal ganglion cells. PLoS One 9, e92105. 10.1371/journal.pone.0092105 [PubMed: 24643061]

Lou H, Kang D, Yang Q, Lian C, Zhang C, Li Z, Tian H, Lu L, Xu GT, Xu G, Zhang J, 2017. Erythropoietin Protects Retina Against Ceramide 2-Induced Damage in Rat. Curr Mol Med 17, 699–706. 10.2174/1566524018666180322161252 [PubMed: 29577857]

McCaffery CA, Raju TR, Bennett MR, 1985. Retinal ganglion cell survival is mediated by cell contact with immature rat astroglia. Neurosci Lett 57, 319–324. 10.1016/0304-3940(85)90512-9 [PubMed: 4034100]

Moreau T, Coles A, Wing M, Isaacs J, Hale G, Waldmann H, Compston A, 1996. Transient increase in symptoms associated with cytokine release in patients with multiple sclerosis. Brain 119 (Pt 1), 225–237. 10.1093/brain/119.1.225 [PubMed: 8624684]

Morgan JE, Tribble JR, 2015. Microbead models in glaucoma. Exp Eye Res 141, 9–14. 10.1016/j.exer.2015.06.020 [PubMed: 26116904]

Nakatani K, Chen C, Koutalos Y, 2002. Calcium diffusion coefficient in rod photoreceptor outer segments. Biophys J 82, 728–739. 10.1016/S0006-3495(02)75435-0 [PubMed: 11806915]

Nishina S, Kohsaka S, Yamaguchi Y, Handa H, Kawakami A, Fujisawa H, Azuma N, 1999. PAX6 expression in the developing human eye. Br J Ophthalmol 83, 723–727. 10.1136/bjo.83.6.723 [PubMed: 10340984]

O'Sullivan ML, Punal VM, Kerstein PC, Brzezinski J.A.t., Glaser T, Wright KM, Kay JN, 2017. Astrocytes follow ganglion cell axons to establish an angiogenic template during retinal development. Glia 65, 1697–1716. 10.1002/glia.23189 [PubMed: 28722174]

Ohlemacher SK, Iglesias CL, Sridhar A, Gamm DM, Meyer JS, 2015. Generation of highly enriched populations of optic vesicle-like retinal cells from human pluripotent stem cells. Curr Protoc Stem Cell Biol 32, 1H 8 1–20. 10.1002/9780470151808.sc01h08s32

Ohlemacher SK, Sridhar A, Xiao Y, Hochstetler AE, Sarfarazi M, Cummins TR, Meyer JS, 2016. Stepwise Differentiation of Retinal Ganglion Cells from Human Pluripotent Stem Cells Enables Analysis of Glaucomatous Neurodegeneration. Stem Cells 34, 1553–1562. 10.1002/stem.2356 [PubMed: 26996528]

Quigley HA, Green WR, 1979. The histology of human glaucoma cupping and optic nerve damage: clinicopathologic correlation in 21 eyes. Ophthalmology 86, 1803–1830. 10.1016/j.ophtha.2020.01.035 [PubMed: 553256]

Ramadan RT, Ramirez R, Novosad BD, Callegan MC, 2006. Acute inflammation and loss of retinal architecture and function during experimental Bacillus endophthalmitis. Curr Eye Res 31, 955–965. 10.1080/02713680600976925 [PubMed: 17114121]

Ramos B, Lahti JM, Claro E, Jackowski S, 2003. Prevalence of necrosis in C2-ceramide-induced cytotoxicity in NB16 neuroblastoma cells. Mol Pharmacol 64, 502–511. 10.1124/mol.64.2.502 [PubMed: 12869656]

Resnikoff S, Pascolini D, Etya'ale D, Kocur I, Pararajasegaram R, Pokharel GP, Mariotti SP, 2004. Global data on visual impairment in the year 2002. Bull World Health Organ 82, 844–851. https://www.ncbi.nlm.nih.gov/pmc/articles/PMC2623053/ [PubMed: 15640920]

Samsel PA, Kisiswa L, Erichsen JT, Cross SD, Morgan JE, 2011. A novel method for the induction of experimental glaucoma using magnetic microspheres. Invest Ophthalmol Vis Sci 52, 1671–1675. 10.1167/iovs.09-3921 [PubMed: 20926815]

Sanvicens N, Cotter TG, 2006. Ceramide is the key mediator of oxidative stress-induced apoptosis in retinal photoreceptor cells. J Neurochem 98, 1432–1444. 10.1111/j.1471-4159.2006.03977.x [PubMed: 16923157]

Sappington RM, Carlson BJ, Crish SD, Calkins DJ, 2010. The microbead occlusion model: a paradigm for induced ocular hypertension in rats and mice. Invest Ophthalmol Vis Sci 51, 207–216. 10.1167/iovs.09-3947 [PubMed: 19850836]

Savinova OV, Sugiyama F, Martin JE, Tomarev SI, Paigen BJ, Smith RS, John SW, 2001. Intraocular pressure in genetically distinct mice: an update and strain survey. BMC Genet 2, 12. 10.1186/1471-2156-2-12 [PubMed: 11532192]

Sawada M, Imamura K, Nagatsu T, 2006. Role of cytokines in inflammatory process in Parkinson's disease. J Neural Transm Suppl, 373–381. 10.1007/978-3-211-45295-0_57 [PubMed: 17017556]

Shi M, Kumar SR, Motajo O, Kretschmer F, Mu X, Badea TC, 2013. Genetic interactions between Brn3 transcription factors in retinal ganglion cell type specification. PLoS One 8, e76347. 10.1371/journal.pone.0076347 [PubMed: 24116103]

Sluch VM, Chamling X, Liu MM, Berlinicke CA, Cheng J, Mitchell KL, Welsbie DS, Zack DJ, 2017. Enhanced Stem Cell Differentiation and Immunopurification of Genome Engineered Human Retinal Ganglion Cells. Stem Cells Transl Med 6, 1972–1986. 10.1002/sctm.17-0059 [PubMed: 29024560]

Sluch VM, Zack DJ, 2014. Stem cells, retinal ganglion cells and glaucoma. Dev Ophthalmol 53, 111–121. 10.1159/000358409 [PubMed: 24732765]

Strettoi E, Gargini C, Novelli E, Sala G, Piano I, Gasco P, Ghidoni R, 2010. Inhibition of ceramide biosynthesis preserves photoreceptor structure and function in a mouse model of retinitis pigmentosa. Proc Natl Acad Sci U S A 107, 18706–18711. 10.1073/pnas.1007644107 [PubMed: 20937879]

Tanaka T, Yokoi T, Tamalu F, Watanabe S, Nishina S, Azuma N, 2016. Generation of Retinal Ganglion Cells With Functional Axons From Mouse Embryonic Stem Cells and Induced Pluripotent Stem Cells. Invest Ophthalmol Vis Sci 57, 3348–3359. 10.1167/iovs.16-19166 [PubMed: 27367502]

Tarkowski E, Andreasen N, Tarkowski A, Blennow K, 2003. Intrathecal inflammation precedes development of Alzheimer's disease. J Neurol Neurosurg Psychiatry 74, 1200–1205. 10.1136/jnnp.74.9.1200 [PubMed: 12933918]

Tezel G, Wax MB, 2000. Increased production of tumor necrosis factor-alpha by glial cells exposed to simulated ischemia or elevated hydrostatic pressure induces apoptosis in cocultured retinal ganglion cells. J Neurosci 20, 8693–8700. 10.1523/JNEUROSCI.20-23-08693.2000 [PubMed: 11102475]

VanderWall KB, Vij R, Ohlemacher SK, Sridhar A, Fligor CM, Feder EM, Edler MC, Baucum AJ 2nd, Cummins TR, Meyer JS, 2019. Astrocytes Regulate the Development and Maturation of Retinal Ganglion Cells Derived from Human Pluripotent Stem Cells. Stem Cell Reports 12, 201–212. 10.1016/j.stemcr.2018.12.010 [PubMed: 30639213]

Wahlin KJ, Maruotti J, Zack DJ, 2014. Modeling retinal dystrophies using patient-derived induced pluripotent stem cells. Adv Exp Med Biol 801, 157–164. 10.1007/978-1-4614-3209-8_20 [PubMed: 24664693]

Wang SW, Kim BS, Ding K, Wang H, Sun D, Johnson RL, Klein WH, Gan L, 2001. Requirement for math5 in the development of retinal ganglion cells. Genes Dev 15, 24–29. doi: 10.1101/gad.855301 [PubMed: 11156601]

Weir J, Rivolta M, Holley M, 2000. Identification of differentiating cochlear hair cells in vitro. Am J Otol 21, 130–134. 10.1016/s0196-0709(00)80087-3 [PubMed: 10651447]

Wu BX, Fan J, Boyer NP, Jenkins RW, Koutalos Y, Hannun YA, Crosson CE, 2015. Lack of Acid Sphingomyelinase Induces Age-Related Retinal Degeneration. PLoS One 10, e0133032. 10.1371/journal.pone.0133032 [PubMed: 26168297]

Yan X, Tezel G, Wax MB, Edward DP, 2000. Matrix metalloproteinases and tumor necrosis factor alpha in glaucomatous optic nerve head. Arch Ophthalmol 118, 666–673. 10.1001/archopht.118.5.666 [PubMed: 10815159]

Yang P, Hernandez MR, 2003. Purification of astrocytes from adult human optic nerve heads by immunopanning. Brain Res Brain Res Protoc 12, 67–76. 10.1016/s1385-299x(03)00073-4 [PubMed: 14613807]

Yoshida S, Yoshida A, Ishibashi T, 2004. Induction of IL-8, MCP-1, and bFGF by TNF-alpha in retinal glial cells: implications for retinal neovascularization during post-ischemic inflammation. Graefes Arch Clin Exp Ophthalmol 242, 409–413. 10.1007/s00417-004-0874-2 [PubMed: 15029502]

You Y, Gupta VK, Li JC, Al-Adawy N, Klistorner A, Graham SL, 2014. FTY720 protects retinal ganglion cells in experimental glaucoma. Invest Ophthalmol Vis Sci 55, 3060–3066. 10.1167/iovs.13-13262 [PubMed: 24744204]

Yuan L, Neufeld AH, 2000. Tumor necrosis factor-alpha: a potentially neurodestructive cytokine produced by glia in the human glaucomatous optic nerve head. Glia 32, 42–50. 10.1002/1098-1136(200010)32:1<42::AID-GLIA40>3.0.CO;2-3 [PubMed: 10975909]

Highlights:

- C2-ceramide can induce RGC death directly
- C2-ceramide can induce RGC death indirectly via the secretion of cytokines from astrocytes
- ASMase inhibition prevents ocular hypertension-induced RGC degeneration

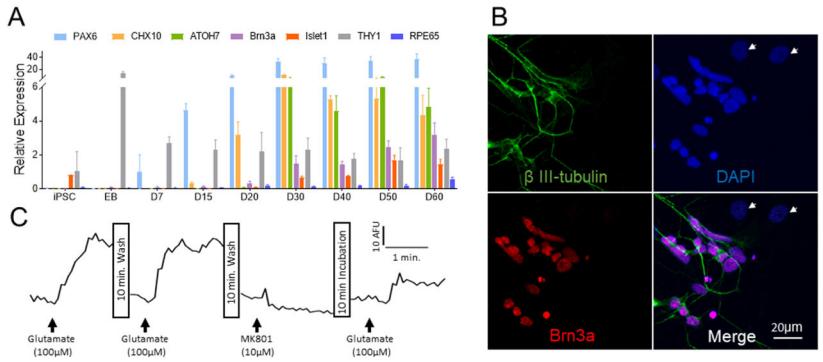

Figure 1. Human iPSC-derived RGCs express RGC markers and respond to glutamate

(A) RT-PCR analyses of iPSCs cells following 60 days of differentiation. Expression of proteins is shown relative to GAPDH. (B) Immunofluorescence staining of purified RGC culture with RGC marker Brn3a- (Red) and neuronal marker beta III-tubulin (Green). Nuclei were stained with DAPI (blue). Cells indicated by arrows are Brn3a or tubulin negative and, therefore, not ganglion cells. (C) Physiological analysis of iPSC-derived RGCs. Ca^{2+}-dependent fluorescence changes in purified RGCs treated with glutamate and MK801.

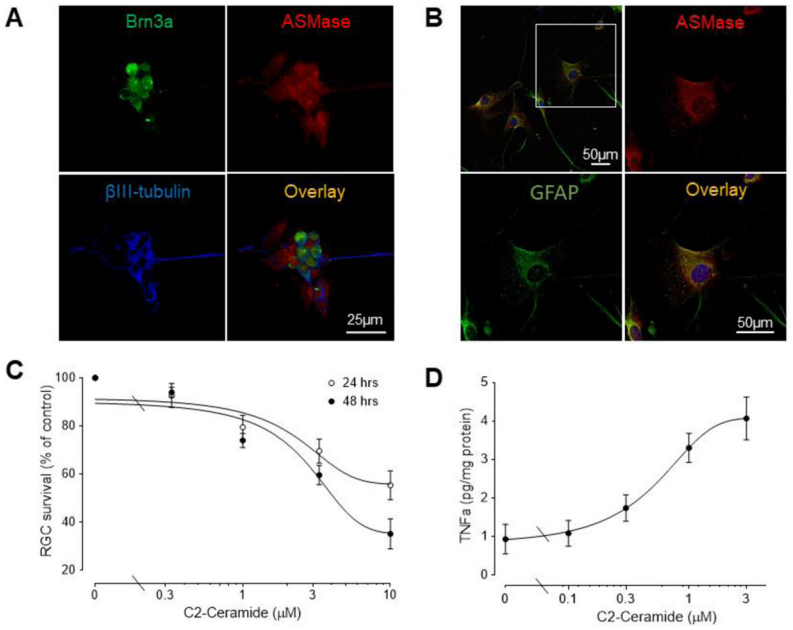

Figure 2. C2-ceramide decreases iPSC-RGC numbers and increases astrocyte TNF- α secretion.

(A) Localization of ASMase in human iPSC-derived RGCs. Immunofluorescence staining of Brn3a (green), ASMase (red), βIII-tubulin (blue) and overlay images. Scale bar, 25 μm. (B) Localization of ASMase in primary cultured human astrocytes. Immunofluorescence staining of GFAP (green), ASMase (red), and overlay images. Scale bar, 25 μm. (C) Survival assay of RGCs treated with C2-ceramide for 24 or 48 hours. Results were normalized to the cell numbers of vehicle-treated controls. Data are mean ± SEM, n≥4. (D) Effect of the C2-ceramide on TNF-α secretion in astrocytes. Cells were treated for 6 hours and media then collected and analyzed. Data are mean ± SEM; $n \geq 4$.

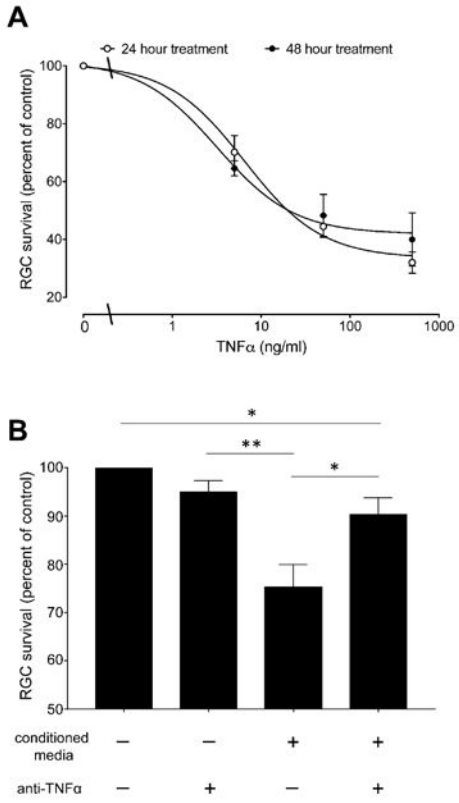

Figure 3. Ceramide-induced secretion of TNF-α by astrocytes leads to reduced iPSC-RGC numbers.

(A) Viability assay of RGCs treated with TNFα for 24 or 48 hours. Results were normalized to the cell numbers of vehicle-treated controls. Data are mean ± SEM, n≥3. (B) Effect of the astrocytes conditioned medium in RGCs. Astrocytes were treated with 10μM C2-ceramide for 24 hours, then media were collected and used for culturing purified RGCs with or without human TNF-α antibody for 24 hours. Data are mean ± SEM; $n \geq 6$. Significant differences indicated as * ($P < 0.05$) or ** ($P < 0.001$), two tailed Student t test.

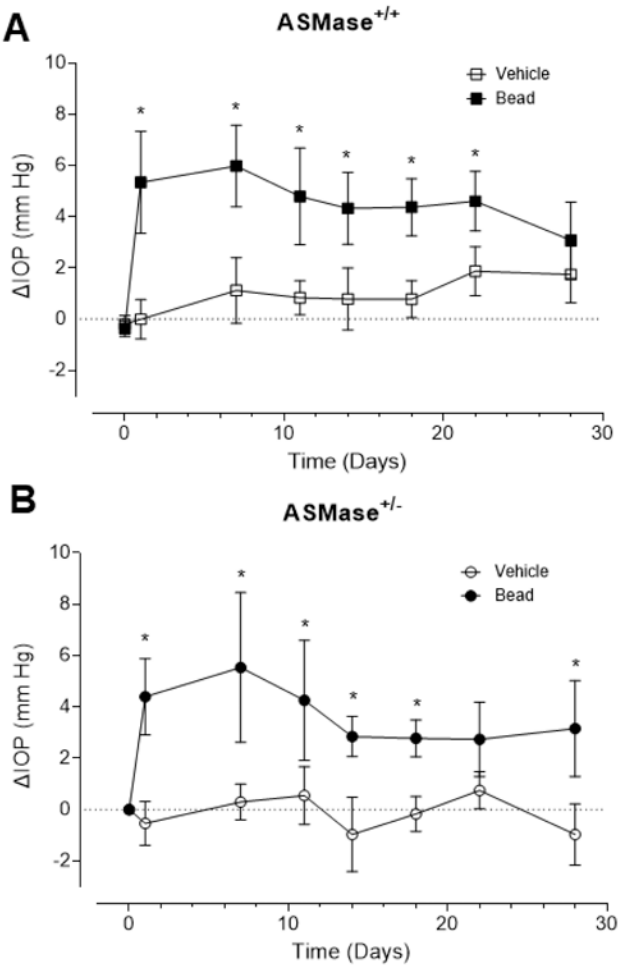

Figure 4. Elevation of IOP following microbead injections in ASMase$^{+/+}$ and ASMase$^{+/-}$ mice.

Comparisons of the change in IOPs from baseline in vehicle- and microbead-injected eyes in (A) ASMase$^{+/+}$ and (B) ASMase$^{+/-}$ mice. ΔIOP is the change in IOP at different time points from the baseline IOP before injection. Data are expressed as mean ± SEM. Significant differences indicated as* ($P < 0.05$, two-tail Student *t* test).

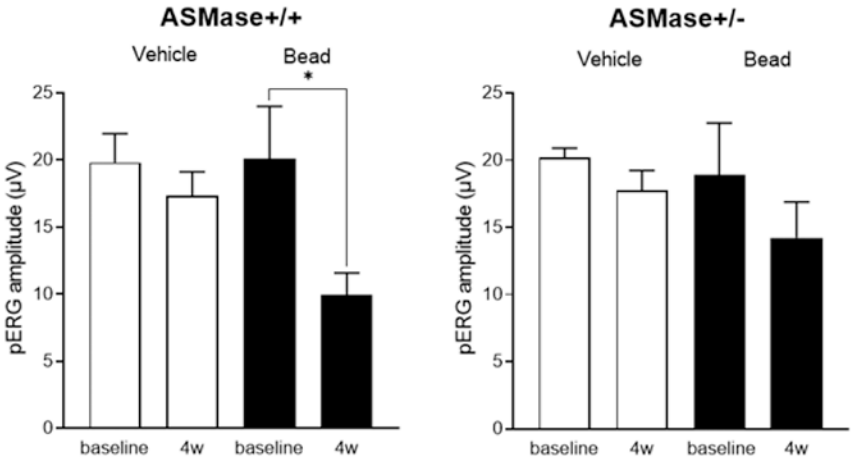

Figure 5. Preservation of RGC pERG response in hypertensive ASMase$^{+/-}$ mice.

Data analysis of the pERG amplitudes of WT and ASMase$^{+/-}$ vehicle and bead-injected eyes before and 4 weeks after the injections. Data are expressed as mean ± SEM. Significant differences indicated as* ($P < 0.05$, two-tail Student *t* test).

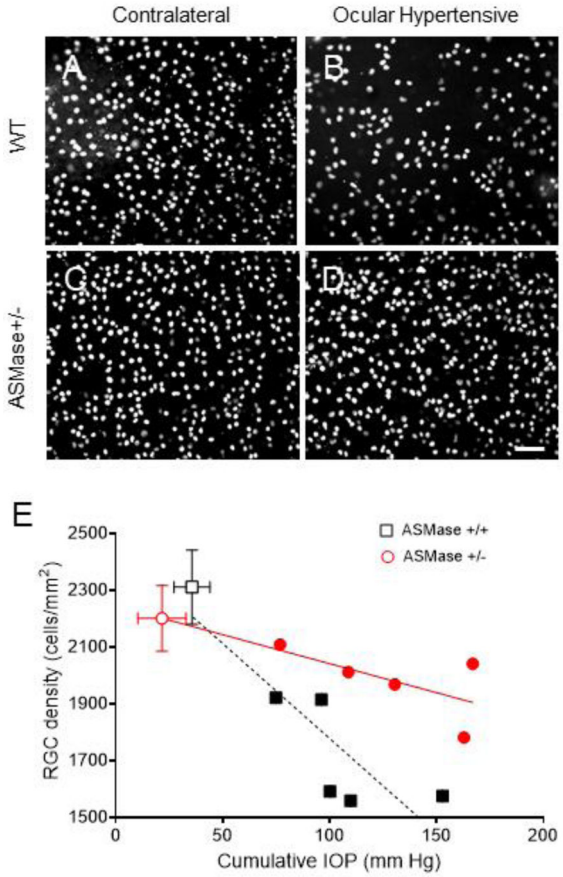

Figure 6. Increased survival of RGCs in ASMase$^{+/-}$ mice with increased IOP.

Representative photograph of Brn3a-labeled retinal ganglion cells in the peripheral mouse retinas. (A) WT control eyes; (B) WT ocular hypertensive eyes; (C) ASMase$^{+/-}$ control eyes and (D) ASMase$^{+/-}$ ocular hypertensive eyes. Scale bar, 50 μm. (E) Correlation of cumulative ΔIOP for 28 days with RGC density in WT (squares) and ASMase$^{+/-}$ mice (circles). Contralateral WT (open square) and ASMase$^{+/-}$ eyes (open circle) are presented as averages. Ocular hypertensive WT eyes (closed square) and ASMase$^{+/-}$ eyes (closed circle) are presented individually. Data are expressed as mean ± SEM. Statistical analysis was performed using unpaired two tailed t test.